SRK House
265 Oxford Road
Illovo 2196
P O Box 55291
Northlands 2116
South Africa
T: +27 (0) 11 441 1111
E: johannesburg@srk.co.za
www.srk.co.za

31 October 2025
605368

Principal Geologist
SRK Consulting South Africa (Pty) Ltd
265 Oxford Road
Illovo,
Johannesburg
2196

Attention: Paul-Johan Aucamp

Dear Paul-Johan,

605368: Longonjo TSF

1. Introduction and Scope of Report

SRK Consulting (Pty) Ltd (SRK) was appointed to conduct a probabilistic seismic hazard assessment (PSHA) for the proposed Longonjo TSF in Angola.

This letter report outlines the seismotectonic review, which is the initial step in the PSHA. The full PSHA report will follow once the site geophysics has been analysed, since the geophysics field results will inform the magnitude of the site correction that will be applied to the results from the PSHA.

1.1. Seismotectonic Review

1.1.1. Tectonic and Geological Framework

The project site in Angola lies within the Congo craton, which is considered a stable continental region (Neto et al., 2018).

The cratons are the oldest known rocks, and have undergone significant changes, with most of the older rocks overlain by younger rocks (Neto et al., 2018). The major tectonic-magmatic cycles that occur within Angola correspond to the Upper and Lower Archaic intervals (ENAGM, cited in Neto et al., 2018). The Lower Archaic (>3 000 Ma) includes gneisses and biotitic plagiogneisses, biotitic hornblendite with biotitic and garnet schists, which are within subordinate biotitic-and bi-micaceous-amphibolite, amphibolite, quartzite, and leptite. The Upper Archaic (2 900 – 2 600 Ma) comprises metasedimentary rocks with amphibolite facies of metamorphism, epidote-amphibolite, and green shales (Neto et al., 2018). Within Angola, the Lower includes the crystalline shield (basement), and the Upper, which covers the platform, includes complexes of the Late Proterozoic, Palaeozoic, Mesozoic, and Cenozoic (Neto et al., 2018), and is shown in Figure 1-1.

Within Angola, the basement outcrops include: (a) Maiombe Shield (Maiombe craton), (b) Angola Shield (Angola craton), (c) Cassai Shield (Cassai craton), (d) Bangwelo Shield (Bangwelo craton), (e) Kwanza Horst, (f) Crystalline rock outcrops in northern and southwestern Angola, and (g) structures of the Upper Proterozoic Shield, greenstone belts, and blocks of primitive continental crust (Neto et al., 2018).

Neto et al. (2018) describe the structures of the platform coverage in Angola, which include the Congo Sedimentary Basin and the Kwanza Sedimentary Basin (structures of the early Mesozoic-Cenozoic (< 230 Ma)), and tectonic-magmatic reactivation of the platform zones. The tectonic-magmatic reactivation zones include: (a) basic magmatism, alkaline, and acid intrusion of Late Riphean, (b) a variety of alkaline-ultrabasic, basic, and alkaline composition intrusive rocks, kimberlite, and carbonatite of Mesozoic, and (c) basalt, dolerite, granite-porphyries, and rhyolite intrusions of Meso-Cenozoic.

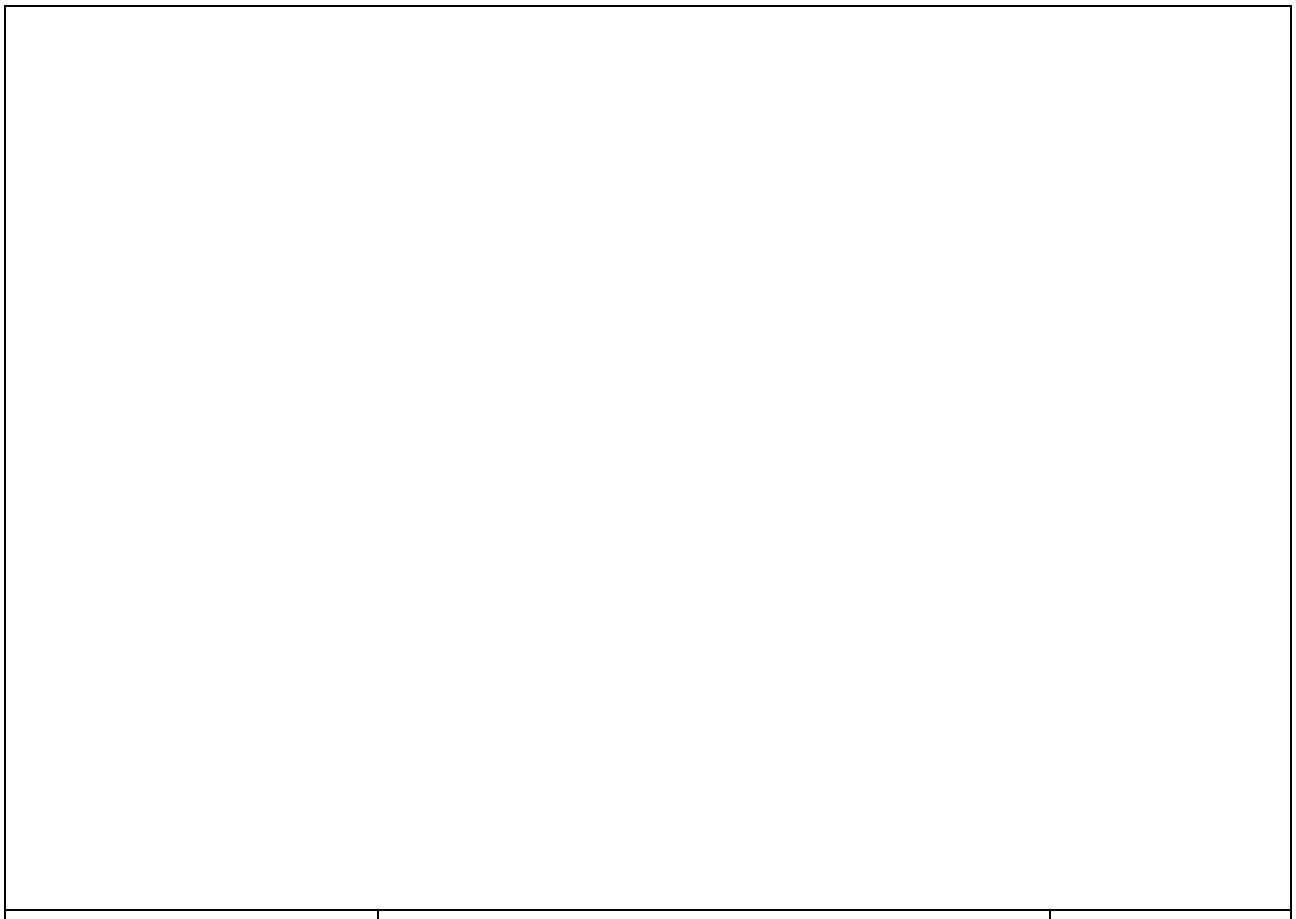

Figure 1-1: Angola geologic map, with the main geological provinces (Neto et al., 2018). The project site is located within the Angola craton (1) and is shown by a yellow star.

West Gondwana (Africa and South America combined) formed in the Neoproterozoic (600 Ma) by the Panafrican and Brazilian orogenies (Trompette, 1994, 1997; Alkmim et al., 2006, cited in Guiraud et al., 2010). Due to rifting (ca. 1.2 Ga), subsequent collision, and obduction (ca. 0.6 Ga) of 2-Ga-old high-grade gneisses, the Panafrican fold belt was formed (Matos, 1992; Feybesse et al., 1998, cited in Guiraud et al., 2010). East-west oblique transpressional collisions and, thereafter, north-south high-angle collision between the African (Congo and Kalahari cratons) and South American (Rio de La Plata, Sao Francisco) parts, formed the final phase of the amalgamation of West Gondwana

(Goscombe and Gray, 2008, cited in Guiraud et al., 2010). In North Angola, the West Congolian Panafrican Mobile Belt is a Neoproterozoic intra-continental rift that inverted ca. 560 Ma ago (Tack et al., 2001, cited in Guiraud et al., 2010). The Angola craton is one of many Archaean blocks that compose the Congo craton and covers most of southwestern and central Angola (Schirbel et al., 2024).

The Angola craton can be subdivided into three main tectonic zones: (a) the Archaean central craton, (b) the Eburnian central craton, and (c) the Coastal Polyorogenic zone of Archaean and Palaeo-Mesoproterozoic granitoid rocks, which were reworked during the Panafrican event (Heilbron et al., 2008, cited in Guiraud et al., 2010). The Archaean central craton and Eburnian central craton, relative to the project site, are shown in Figure 1-2. The Archaean central craton comprises a gneiss-migmatite-granite complex and a gabbro-norite and charnockitic unit, and the Eburnian central craton outcrops along the southern onshore Angolan margin. The Eburnian central craton comprises granitoid suites, granite-gneisses, and metavolcano-sedimentary sequences (Guiraud et al, 2010).

	LONGONJO TSF KWANZA AND BENGUELA BASIN STRUCTURAL MAP	Project No. 605368

Figure 1-2: Structural map of the Kwanza and Benguela rift basins and surrounding basement areas (Guiraud, et al., 2010). The location of the project site (red star) within the Angolan craton (Eburnian granitoids and gneisses).

Continental rifting of the African and South American plates, initiating the South Atlantic Ocean, started around 140 Ma in Argentina with east-west-oriented rifts (Davison, 1999; Macdonald et al., 2003, cited in Guiraud et al., 2010) and in the northern rifts: Reconcavo, Sergipe-Alagoas, Potiguar (Davison, 1999, cited in Guiraud et al., 2010), Gabon and Benue (Guiraud, 1990, 1993; Teisserenc and Villemin, 1990; Mbina Mounguengui and Guiraud, 2009, cited in Guiraud et al., 2010). The subsequent progressive widening of the South Atlantic by plate accretion continues today (Sibuet et al., 1984; Schlumberger, 1991; Brandão, 2003, cited in Neto et al., 2018) (age of oceanic crust shown in Figure 1-3). Barremian (Early Cretaceous) rifting started along the whole margin around 130-125 Ma (Davison, 1999, cited in Guiraud et al., 2010). Under the influence of northeast-southwest-oriented extensional palaeostresses, rift basins of the West and Central African rift system opened and became part of the South Atlantic coastal rift system (Reyre, 1984; Matos, 1992; Mascle et al., 1993; Maurin and Guiraud, 1993, cited in Guiraud et al., 2010). The active rift sequence of the Kwanza and Cabinda areas (North Angola) is of Neocomian and Barremian age (Braccini et al., 1997; Bate et al., 2001, cited in Guiraud et al., 2010). In the onshore Kwanza Basin, rifting is associated with normal faulting associated with the basement (Lima Neeves, 1999; Bate et al., 2001, cited in Guiraud et al., 2010). Syn-rift deposits are subdivided into three main lithostratigraphic units: (a) Red Cuvo, (b) Grey Cuvo, and (c) Cuvo-Chela, bound by erosional unconformities (Brognon and Verrier, 1966; Henry et al., 1995; Bate et al., 2001, cited in Guiraud et al., 2010).

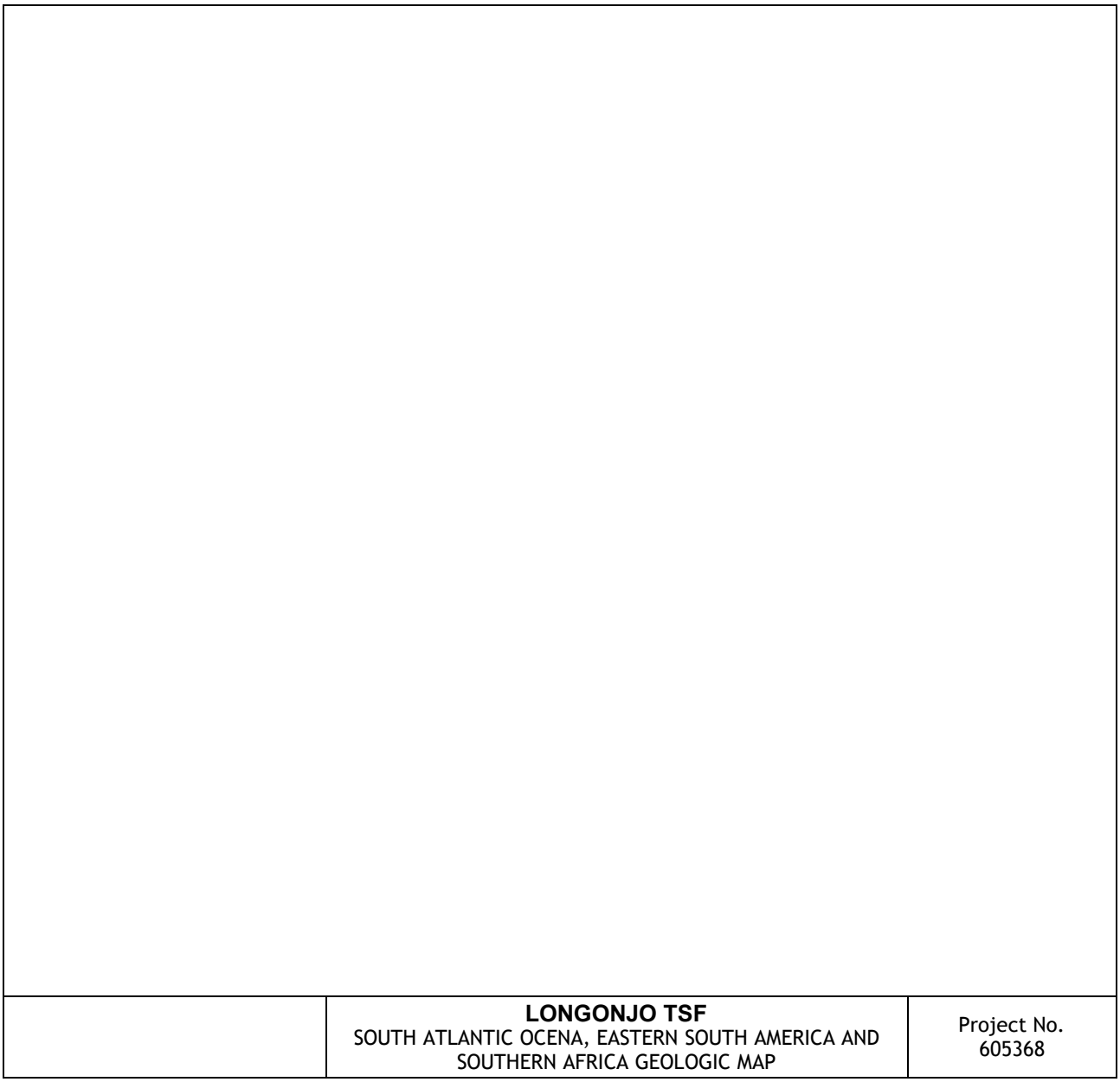

Figure 1-3: Geologic map of the South Atlantic Ocean, Eastern South America, and Southern Africa. Onshore, the Main Paleoproterozoic cratonic shields are outlined in thick black and encompass their internal Archean nuclei, shown in dark pink. Offshore, major oceanic fracture zones are shown in dashed black lines, compartmentalising the different segments of the South Atlantic Ocean. Secondary fracture zones are shown in grey lines (Escosa, et al., 2024). The location of the project site (red star) within the Congo cratonic shield relative to the Mid-Atlantic Ridge (pink lines) and oceanic fracture zones.

Post-rifting, from Late Barremian to Early Aptian, the Aptian marine transgression led to the sedimentation of the massive salt (Loeme) Formation (Guiraud et al., 2010). In the Kwanza Basin (shown in Figure 1-2), the Upper Cretaceous is affected by a gravitational extension of the post-rift succession over the underlying Aptian evaporites (Duval et al., 1992; Jackson et al., 2005, cited in Guiraud et al., 2010). The Santonian (Late Cretaceous) to Eocene sedimentation is composed of aggrading to retrograding clastic sediments interlayered with a proportion of carbonates (Anderson et al., 2000, cited in Guiraud et al., 2010). A wide prograding clastic wedge, which is disrupted by major erosions at the regional scale on the platform and coastal plain of the margin (Duval et al., 1992; Spathopoulos, 1996; Fort et al., 2004; Jackson et al., 2005, cited in Guiraud et al., 2010), is evidence of the post-Oligocene period of lowstand icehouse-induced conditions and inner margin uplift (Lunde

et al., 1992; Marton et al., 2000; Seranne and Anka, 2005, cited in Guiraud et al., 2010). Depositional loading by clastics derived from the uplifted areas intensified Cenozoic gravity-induced rafting of slabs of the post-salt succession downdip along the Aptian salt decollement, therefore generating upslope extensional structures (pre-rafts, rafts), diapirs, and downslope contractional features (folds and allochthonous sheets) in offshore domains (Duval et al., 1992; Lundin, 1992; Spathopoulos, 1996; Marton et al., 2000; Fort et al., 2004, cited in Guiraud et al., 2010).

According to Sibuet et al. (1984), cited in Neto et al. (2018), seismic data and Deep Sea Drilling Project holes drilled in the passive continental margin were used to define tectonostratigraphic units and have been related to three main evolution stages of the continental margins: (I) the pre-rift sequence, (II) the syn-rift sequence, and (III) the post-rift sequence. The pre-rift sequence corresponds to the continental basement but includes volcanic and sedimentary sequences deposited before the tensional movements that resulted in the formation of the continental margin. The syn-rift sequence is related to strong tectonics that corresponds to the rifting phase, and it is thought that the continental crust thinned during this tensional phase. The post-rift sequence correlates to when oceanic crust was emplaced at the end of the rifting phase, which, thereafter, subsidence of the continental margin was thermally affected and corresponds to the tilting around the initial hinge line.

Based on the existence of distinct structural-stratigraphic styles, Brice et al. (1982) and Karner et al. (1997), cited in Neto et al. (2018), identified five different tectonic episodes: (I) pre-rift (Jurassic) characterised by soft tectonics, (II) syn-rift I (Neocomian to lower Barremian) characterised by strong tectonism, (III), syn-rift II (Barremian to Aptian) with moderate tectonism, (IV) post-rift (Albian to Eocene), corresponding to continental drift phase associated with weak tectonism, and (V) regional subsidence (Oligocene to Holocene), characterised by the tilting of the basins westward.

According to Guiraud et al. (2010), cited in Neto et al. (2018), the Angola margin comprises three sub-basins: (a) the North Kwanza margin segment that opened into the West Congolian Panafrican Mobile Belt; (b) the South Kwanza margin segment, and (c) the Benguela margin segment. The South Kwanza and Benguela margin segments formed along the narrow coastal Panafrican mobile belt, which is on the western edge of the Angola Eburnian craton (Figure 1-2). Tectonic features of the Panafrican fold belt include westward-dipping mylonitic shear zones, which suggest Early Cretaceous coastal rift systems of Angola opened along weak zones in the Precambrian crust.

Within the West Congolian Panafrican Mobile Belt, a NW-SE syn-rift fault grain that is parallel to the basement fabric is present in the North Kwanza orthogonal rift (Guiraud et al., 2010, cited in Neto et al., 2018). The fold-and-thrust terranes of the West-Congo Belt host large, NE-SW, NW-SW, and N-S trending brittle shear zones (Alvarez & Maurin, 1991; Nkodia et al., 2021, cited in Nkodia et al., 2022). Early Palaeozoic sandstones cover the terranes of the mobile belt and have two main phases of strike-slip deformation, the first being during the Gonwanide Orogeny in the Permo-Triassic, and the second during the Cretaceous opening of the Atlantic (Miyouna et al. 2018; Nkodia et al., 2021, cited in Nkodia et al., 2022). The syn-rift faults of the North Kwanza coastal rift trend in a 140°-150° direction and correspond to the Early Cretaceous reactivation along the pre-existing Panafrican low-angle thrust planes of the West Congolian fold belt. Within the South Kwanza oblique rift, the 170°-010° trending rift faults and associated Porto Amboin intracontinental transfer faults are controlled by the reactivation of the major Precambrian ENE-WSW shear zones of the Kwanza Horst and second-order Eburnian Paleoproterozoic (170°-010° trending) fractures that cross-cut the Angolan Shield. The Kwanza Horst is a major crustal discontinuity between the Upper Proterozoic West Congolian fold belt and the Eburnian Paleoproterozoic Angolan shield. Within the Benguela coastal rift, transform rifting and the associated major 050° Cuio transform fault were formed at a low angle to the NE-trending boundary between the Panafrican mobile belt and the Angola craton (Guiraud et al., 2010, cited in Neto et al., 2018).

1.1.2. Seismicity

1.1.2.1 Earthquakes – Historical, Instrumental, and Induced

Moreira (1968), cited in Neto et al. (2018), reported approximately 129 earthquakes, most of which were of relatively low intensity, that were felt in Angola from 1945 to 1965, including earthquakes with intensities VI-VII on the Mercalli-Cancani-Sieberg scale. After 1965, the war for Angolan independence intensified, and during the civil war, which lasted until 2002, the seismic work in Angola stopped. In 2003, the Angolan Instituto Nacional de Geofísica e Meteorologia (INAMET) and Agostinho Neto University (UAN) restarted monitoring and reporting seismic activity (Neto et al., 2018).

Neto et al. (2018) reported 116 events with magnitudes between 2.6 and 6.0 from 1914 to March 2014 from the ISC Bulletin, and 12 events with magnitudes between 3.9 and 5.3 m_b between 1976 to 2013 from the USGS Bulletin for Angola, with all events from the USGS Bulletin being included in the ISC Bulletin.

Neto et al. (2018) fitted the Angolan earthquakes to the Gutenberg-Richter relation ($\log N = a - b\,M$), where N is the number of earthquakes of magnitude M and higher and a and b are constants for a certain region (Richter, 1958, cited in Neto et al., 2018), and yielded an estimated regional b value of 0.66±0.06, and a completeness magnitude of 3.0 for 177 events. According to Neto et al. (2018), the b value was quite low, which is characteristic of stable continental regions (SCR) (Talwani et al.,2017, cited in Neto et al., 2018).

The largest known event to have occurred in Angola appears to be a M_S 6.0 earthquake in 1914 (International Seismological Centre, 2025; Neto et al., 2018), with no macroseismic reports for the event according to Ambraseys and Adams (1991). Recently, three earthquakes within the Angola craton were recorded on the Capanda Seismograph Network (SNC), which the Gabinete de Aproveitamento do Médio Kwanza (GAMEK) has been operating since January 2013 (Neto et al., 2018). Two events occurred on 23 July and 19 November 2013, with magnitudes of 2.2 and 3.9, respectively, and the third event occurred on 10 November 2014 (Neto et al., 2018).

The Cassongue earthquake of magnitude 4.2 mb (International Seismological Centre, 2025)(19 November 2023) and the Balombo earthquake of magnitude 4.1 mb (International Seismological Centre, 2025) (10 November 2014) occurred within the Lucapa Graben. The Lucapa Graben is thought to be a tectonic-magmatic reactivation zone of Mesozoic age, with alkaline, basaltic, and kimberlite intrusions. The distribution of known diamond and nickel deposits is related to the zones of crustal weakness, particularly where two or more zones intersect (Crockett and Mason, 1968, cited in Neto et al., 2018).

The Capanda earthquake of magnitude 2.2 occurred on 23 July 2023, close to the Angola craton edge, which is approximately 17 km away from the Capanda reservoir, which forms part of the Kwanza Horst. The Kwanza Horst is a linear, latitudinal basement elevation, which is 25-50 km wide and approximately 300 km in length, bordered by deep faults in the north and south, and covered by a thin cover of sedimentary deposits of the Upper Proterozoic. The lifting of the Kwanza Horst reached a maximum in the final stage (orogenic) of the Upper Proterozoic cycle (ENAGM, 1988, cited in Neto et al., 2018). The Capanda earthquake can be associated with a preexisting weakness zone and stress concentration (Gangopadhyay and Talwani, 2003, cited in Neto et al., 2018), with the possibility of the earthquake being triggered by the Capanda reservoir if a hydroseismicity model is considered (Neto et al., 2018; Schirbel et al., 2024).

Downstream of the Kwanza River, approximately 40 km from the Capanda dam, is the location of the Laúca reservoir. Impoundment of the Laúca reservoir began in late 2017, and seismicity started in March 2018, shortly after the water level reached 86 m (Schirbel et al., 2024). Impoundment of water reservoirs changes the normal and shear stresses on pre-existing fault planes through both surface

loading and pore pressure changes and serves as a trigger for the release of tectonically accumulated stress (Simpson, 1986; Talwani, 1997, cited in Schirbel et al., 2024). However, the impoundments of the older Capanda reservoir in 2002 showed no discernible change in the natural rate of seismicity in the region (Schirbel et al., 2024). Between March 2018 and April 2024, 287 events were recorded, with the largest being 3.0 M_L that was felt in nearby villages and towns (Schirbel et al., 2024). The reservoir area is characterised by predominantly Paleoproterozoic granitic and Neoproterozoic gneissic rocks (Neto, 2014, cited in Schirbel et al., 2024), with a thin sedimentary layer along the Kwanza riverbanks (Schirbel et al., 2024). In addition to induced seismic events, natural events occur in the reservoir area, with the largest known event of magnitude 6.0 M_S in 1914. The 6.0 M_S event occurred 35 km from the dam (Neto, 2014, cited in Schirbel et al., 2024).

The African stress field is largely unmapped through focal mechanisms due to the overall low seismicity in intraplate regions and a lack of adequate network coverage in many areas (Schirbel et al., 2024). Delvaux and Barth (2010), cited in Schirbel et al. (2024), inverted for stress using focal mechanisms over the Nubian and Somalian plates, show that in the Congo Basin and adjacent areas, the continent is in compression, with SH_{max} orientated in the east-west direction, and the majority of earthquakes show either strike-slip or reverse faulting. Schirbel et al. (2024) characterised the seismicity induced at the Laúca reservoir, which suggests strike-slip faulting, with a NE-SW deviatoric compression. Faulting changes from reverse faulting in the Congo Basin to strike-slip at the Laúca reservoir and then to normal faulting in Northern Namibia, with the SH_{max} changing from E-W to NE-SW to NNW-SSE (Schirbel et al., 2024).

According to Guiraud et al. (2010), multiple, large (magnitude 4-5) seismic events occurred on the western slope of the southern Angola escarpment (i.e., coastal bulge), and this is evidence for the Recent differential uplift of the inner domain of the Angola margin and suggests that deformation is ongoing in the present day. Guiraud et al. (2010) derived east-west to northeast-trending main horizontal stresses that are associated with thrust faulting or strike-slip regimes are restricted to the eastern domains of Gabon and Angola. NNW-trending horizontal stresses causing normal faulting are located in the southwestern domain of Angola. A broad domain of Angola is affected by a NW-NNW compressive horizontal stress (Viola et al., 2005, cited in Guiraud et al., 2010). In the present-day NW-NNW compressional state, and assuming this stress has been long-term, the Benguela margin, which is a NE-trending transform, is largely normal to the NW-NNW horizontal compressive stress and is likely to accommodate major recent uplift and associated thrust faulting. However, the NNW-trending orthogonal-rifted Kwanza margin is at an acute angle to the NW-NNW horizontal compressive stress and probably accommodates less Recent uplift and transtensive to transpressional faulting (Guiraud et al., 2010).

1.1.2.2 Potential Seismogenic Sources and Seismogenic Zones

Fault Reactivation

The Angolan (or Bié) Dome is centred on Angola (Sahagian, 1988; Burke and Gunnell, 2008, cited in Klöcking et al., 2020), and occurs along the Angolan coastline between 9° and 16° south, comprising portions of the Kwanza and Benguela Basins, to the north and south, respectively (Klöcking et al., 2020). The Angolan Dome is a zone of localised mantle upwelling (Reusch et al., 2010; Walker et al., 2016, cited in Nkodia et al., 2022), driving magmatic activities and associated earthquakes (De Plaen et al., 2014; Tabod et al., 1992; Ubangoh et al., 1997, cited in Nkodia et al., 2022), and some events occurring around the Dome according to Nkodia et al. (2022). Infrequent and low-magnitude seismic events occur around the Dome, with less than five recorded earthquakes with M_w > 5 (CMT Catalog; Diziewonski et al., 1981, cited in Klöcking et al., 2020). Focal mechanism solutions and fault scarps show predominantly extensional or strike-slip motion, with tectonic activity appearing to be limited to reactivated, deep lineaments that trend in a northeast-southwest direction, along the remnant

extensional graben, known as the Lucapa corridor (Almeida et al., 1981; Sykes, 1978, cited in Klöcking et al., 2020).

According to Nkodia et al. (2022), the regional clustering of earthquakes along and in the proximity of preexisting tectonic lineaments, and the stress analysis performed, indicate that earthquakes along the continental margin of western Africa and western Central Africa are likely associated with seismogenic reactivation of preexisting fault systems inherited from past tectonic events. Nkodia et al. (2022) suggest that there is potential for brittle reactivation of preexisting structures based on the clustering of intraplate earthquakes along or around preexisting basement-rooted faults.

According to Nkodia et al. (2022), there is a variation in the stress regime across the coastal margin and inland, with the coastal margin having a strike-slip faulting regime with a minor compressional regime component and, inland, a compressive regime with a moderate strike-slip faulting component, i.e. from a transpressive stress regime (NNE-SSW-oriented maximum horizontal compressive stress (SH_{max})) offshore and near the coastal margins, a compressive stress regime (NE-SW-oriented SH_{max}) in the Congo Basin, to a transtensive stress regime (E-W-oriented SH_{max}) in the Kasai Block of the Congo Craton. In the contemporary stress field, the pre-existing, NNE-, NNW-, and N-S trending strike-slip faults and normal faults show a high slip tendency, which suggests a high likelihood of being reactivated. Nkodia et al. (2022) suggest that due to the transition of the stress regime, the NW-SE to NNE-SE strike-slip faults/normal faults have the highest tendency to be reactivated in the coastal margin area during the past or present day, and within the cratonic interior of western Central Africa, the NW- and N-S trending thrust faults are the most probable structures to be reactivated, with strike-slip faults being less likely. Multiple studies have inferred that preexisting fractures are hosting earthquakes along the continental margins and interior of western Africa; however, there are insufficient details of the ambient stress field and the evidence for coseismic surface fault rupture or the presence of active fault scarps (Amponsah, 2002; Ayele, 2002; Blundell, 1976; Bouka Biona and Sounga, 2001; Kutu, 2013; Olugboji et al., 2021; Sykes, 1978, cited in Nkodia et al., 2022).

According to Nkodia et al. (2022), the structural geometry of preexisting fault zone fracture surfaces is favourably oriented for reactivation in the contemporary stress field, but the fault orientation does not determine whether faults would reactivate by stable creep or seismic rupture. The susceptibility of faults to seismic or stable creep reactivation is determined by the frictional stability of the fault rocks at the contemporary temperature and pressure conditions at depth in the crust (Blanpied et al., 1998; Dieterich, 1979; Ikari et al., 2011; Marone, 1998), cited in Nkodia et al., 2022), which is applicable for active plate boundary settings (Carpenter et al., 2009, cited in Nkodia et al., 2022), and intraplate settings (Kolawole et al., 2019, cited in Nkodia et al., 2022). Nkodia et al. (2022) suggest proposed mechanisms for the origin of stress loading leading to seismogenic rupture of preexisting faults in the onshore areas of western Africa's continental margin, include variations in the lithospheric structure and gravitational potential energy associated with the mid-ocean ridge (Mahatsente and Coblentz, 2016; Medvedev, 2016, cited in Nkodia et al., 2022), post-rift crustal relaxations along the rifted margin, landward continuation of oceanic fracture zones, and induced earthquakes triggered by groundwater extraction (Olugboji et al., 2021, cited in Nkodia et al., 2022).

According to Nkodia et al. (2022), the stress acting on the offshore oceanic fracture zones is comparable with the stress acting along the onshore areas of the continental margin, and the onshore pre-existing strike-slip faults, which are parallel to the oceanic fracture zones, have a high slip tendency in this contemporary stress field. The Romanche, Chain, Charcot, Ascension, and Saint Paul fracture zones are active fracture zones that extend to or into the western Africa rifted continental margin (Heezen et al., 1964, 1965; Mascle and Sibuet, 1974, cited in Nkodia et al., 2022). Intraplate faults could be activated by far-field strain transfer from transform faults along the spreading ridges, considering that some of the oceanic fracture zones are active (Meghraoui et al., 2019, cited in Nkodia et al., 2022). Nkodia et al. (2022) propose that higher stress magnitude zones along the distal offshore

oceanic fracture zones extend into the continent and may be driving stress loading on pre-stress, favourably oriented fault systems onshore, along the continental margin.

Salt Tectonics

During the Early Cretaceous, rifting of the Kwanza Basin was initiated in association with the opening of the South Atlantic Ocean. The rifting occurred in response to NE-oriented extension (Guiraud et al., 2010; Maurin and Guiraud, 1993, cited in Erdi and Jackson, 2022) and was partially accommodated by the formation of NE-trending transform faults (Guiraud et al., 2010, cited in Erdi and Jackson, 2022). According to Erdi and Jackson (2021), cited in Erdi and Jackson (2022), these transform faults bound arrays of rift-related, NE-trending, horst-and graben-structures in the Outer Kwanza basin (seaward of the Kwanza basin). A thick layer of Aptian salt unit was deposited during the latter stage of rifting. This salt layer thickens seaward (i.e., west) and along-strike (i.e., south) (Evans and Jackson, 2021; Von Nicolai, 2011, cited in Erdi and Jackson, 2022), draping relief associated with the underlying rift-related structures (Erdi and Jackson, 2021; Hudec and Jackson, 2004, cited in Erdi and Jackson, 2022). Since the deposition of Aptian salt, salt tectonics has included the tectono-stratigraphic development of the Outer Kwanza Basin, through gravity-driven deformation (Duval et al, 1922; Lundin, 1992; Marton et al., 2000, cited in Erdi and Jackson, 2022), which are linked zones of updip extension above the Flamingo Platform and downdip contractional towards the seaward edge of the salt (Hudec and Jackson, 2004, cited in Erdi and Jackson, 2022).

Erdi and Jackson (2021), cited in Erdi and Jackson (2022), show that although the overburden strike-slip faults have similar strikes and are located spatially within the NE-trending, basement-involved transform fault, they are of different ages and kinematically different systems. The overburden strike-slip faults are post-Aptian and formed to accommodate along-strike differences in salt-related contraction or extension. Edri and Jackson (2022) show that deformation of Albian-to-Recent overburden, above Aptian salt, is accommodated by four, NE-SW-striking fault arrays that are 13 km long, and have normal and reverse throws of up to 617 and 830 m, respectively, and that the thickness variations associated with the fault arrays show that they were active at different times, with two subsets of the arrays still being active.

Seismogenic zones

Neto et al. (2018) have divided Angola into five seismotectonic zones based on evaluating the earthquake density from the earthquake catalogue between 1914 and 2014, as shown in Figure 1-4. The main active zones are defined as (1) Angola craton, where the largest known event to have occurred in this region is a magnitude 6.0 earthquake in 1914, (2) Cassai craton, (3) Bangweulo craton, (4) intracratonic sedimentary basin, and (5) passive margin and Angola offshore. According to Neto et al. (2018), Moreira (1968) delineated the main seismic zones of Angola based on macroseismic data and correlated well with the seismotectonic zones defined by Neto et al. (2018), excluding the passive margin. The project site is located within the seismogenic zone (1), Angola craton.

According to Neto et al. (2018), the three craton zones: Angola, Cassai, and Bangweulo, show that the majority of the macroseismic and instrumental earthquakes epicentres are located within or at the edge of grabens, which cross-cut the cratons. The grabens comprise areas of tectonic-magmatic Meso-Cenozoic reactivation zones, with various intrusive rocks of alkaline-ultrabasic, basic, and alkaline compositions, kimberlite, and carbonatite (Neto et al., 2018). Crockett and Mason (1968), cited in Neto et al. (2018), observed that seismic activity in South Africa is concentrated in a distinct area that approximates the distribution of lava of the Karoo system and the younger kimberlite pipes. According to Dawson (1970), cited in Neto et al. (2018), kimberlites in South Africa, are of Cretaceous age, and are thought to been intruded during a period of strong uplift of the continent with attendant downwarping or faulting around the periphery as a result of the deepening of the contiguous ocean basins and concludes that kimberlites were intruded for the most part into major fundamental fracture that cross-cut cratonic area and the Circum-Cratonic belts during the periods of epeirogenic uplift.

Based on the remarks of Dawson (1970), Neto et al. (2018) propose a similar hypothesis for the seismicity in the craton zones.

Within the intracratonic basin, which is within the transcontinental Okavango Depression: Zambeze (ZBE), Cuando (CDO), and Cubango (CGO) sub-basins, Constain et al. (1987), cited in Neto et al. (2018), hypothesize that earthquakes that occur in this area can be associated with the hydroseismicity model. According to the hydroseismicity model, the seismicity in this region is due to the weakening of rocks due to chemical and mechanical factors that require the presence of seismogenic crustal volume and a large amount of water from rivers and basins to achieve sub-crustal depths, assuming a permeable crust under tectonic stress, close to rupture (Talwani 1989; Talwani and Rajendran 1991, cited in Neto et al., 2018). According to Crosby et al. (2010), cited in Neto et al. (2018), the seismicity suggested mild surface shortening in the Congo Basin.

The seismicity activity in the Angolan passive margin (between the coastline and the 2000-m bathymetric contour) can be associated with flexural stress (Assumpção et al., 2011, cited in Neto et al., 2018). The rifting of the continental margin of Angola synchronously led to a thicker layer. Flexural coupling caused by the subsiding oceanic Angola Basin and the subsiding continental margin occurred in post-Aptian and created a westward thickening wedge of Cretaceous and Cenozoic sediments. The Angola Basin is systematically shallower than the global average, which is typical of the tectonic behaviour of the African Plate, which has a higher regional average elevation than other continents (Neto, et al., 2018). According to Schlumberger (2011), cited in Neto et al. (2018), intraplate earthquakes occur mainly inside the African continental crust for reasons related to the lower vertically integrated strength of the lithosphere when compared to the oceanic lithosphere.

Figure 1-4: Angola seismicity map with five seismic zones (Neto, et al., 2018). The project site (yellow star) is located within the seismogenic zone (1), Angola craton.

1.1.3. Data sources

The magnitude and the prime hypocentre location of historical earthquakes, in this work, were sourced from the ISC Bulletin (International Seismological Centre, 2025) for the period from 1900 to 21 October 2025, in the range of 5°S to 18.5°S latitude, and 10° E to 24.5°E longitude, with any magnitude,

magnitude type, and depth range. For this work, 249 events were sourced from the ISC Bulletin, with the following contributing agencies;

- AUST Geoscience Australia
- AWI Alfred Wegener Institute for Polar and Marine Research
- BCIS Bureau Central International de Sismologie
- BGSI Botswana Geoscience Institute
- BJI China Earthquake Networks Center
- BRA Geophysical Institute, Slovak Academy of Sciences
- BUL Goetz Observatory
- CENT Centennial Earthquake Catalog
- EAF East African Network
- EHB Engdahl, van der Hilst and Buland
- EIDC Experimental (GSETT3) International Data Center
- EVBIB Data from publications listed in the ISC Event Bibliography
- GCMT The Global CMT Project
- GFZ Helmholtz Centre Potsdam GFZ German Research Centre For Geosciences
- IDC International Data Centre, CTBTO
- ISC International Seismological Centre
- ISC-EHB Revision and Continuation of the EHB project
- ISS International Seismological Summary
- JOH Bernard Price Institute of Geophysics
- LDG Laboratoire de Détection et de Géophysique/CEA
- LSZ Geological Survey Department of Zambia
- MCSM Main Centre for Special Monitoring
- MOS Geophysical Survey of Russian Academy of Sciences
- NAM The Geological Survey of Namibia
- NEIC National Earthquake Information Center
- NEIS National Earthquake Information Service
- PRE Council for Geoscience
- USCGS United States Coast and Geodetic Survey
- VAO Instituto Astronomico e Geofísico

Public catalogues, with several contributing agencies, report the magnitude of historical earthquakes on different magnitude scales based on the earthquake size, instruments, and available data of the agency.

The different magnitude scales that are used are described as follows;

- M_L is the original magnitude relationship defined by Gutenberg and Richter in 1944 for local earthquakes (Gutenberg & Richter, 1944).
- M_S is a magnitude based on the amplitude of Rayleigh surface waves measured at a period near 20 sec. It is reported by the National Earthquake Information Centre (NEIC) operated by the United States Geological Survey (USGS), but it is not viewed as authoritative.
- M_w is the moment magnitude and is considered the most objective measure of an earthquake's size in regard to total energy. However, it is based on a simple model of rupture that incorrectly assumes that the proportion of energy radiated as seismic waves is the same for all earthquakes. M_{ww}, M_{wc}, M_{wb}, and M_{wr} are subtypes of M_w and are based on different methods used to calculate the seismic moment tensor.
- The m_b type magnitude stands for short-period body wave and is based on the amplitude of first arriving P-waves at periods of about 1 s. The m_b magnitude is reported for most M 4.0-4.5 to 6.5 earthquakes that are observed teleseismically, and is only authoritative for global seismicity, for which there is no M_{ww}, M_{wc}, M_{wb}, or M_{wr}, typically 4.0-5.5 range. m_b tends to saturate at about M 6.5 or larger.
- M_D is the magnitude based on the duration of shaking and is measured by the time decay of the amplitude of the seismogram. M_D is computed by NEIC but only published when there is no other magnitude available.

For this work, multiple events from the ISC Bulletin had different magnitude scales reported by different agencies for the same event. The magnitude with type M_w was prioritised, and in the absence of M_w, m_b, M_L, M_S, M_D , in that order, was prioritised. In the case of the same event having the same magnitude type but different values reported by different agencies, the higher value is shown in this work. Events that only had one magnitude scale, irrespective of the magnitude type, were included as is.

1.1.4. Seismicity within 500 km of the site

All events recorded from 1900 to 21 October 2025 within a 500 km radius of the project site are shown in Figure 1-1.

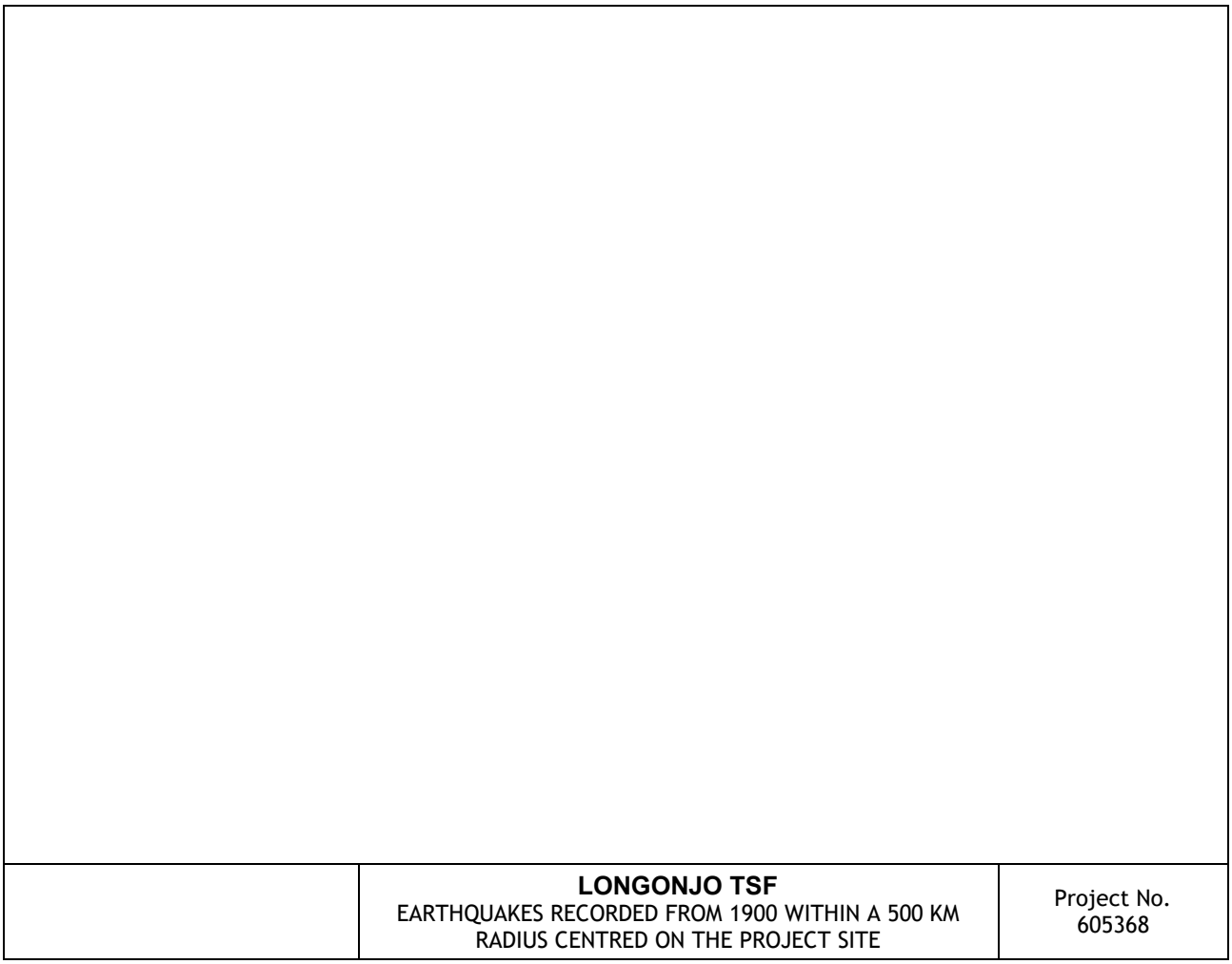

Figure 1-5: Earthquakes recorded from 1900 within a 500 km radius centred on the project site.

All M ≥ 4 events recorded from 1900 to 21 October 2025, within a 500 km radius of the project site, are shown in Figure 1-6. The dates of the event occurrence and hypocentral data are provided in Table 1-1.

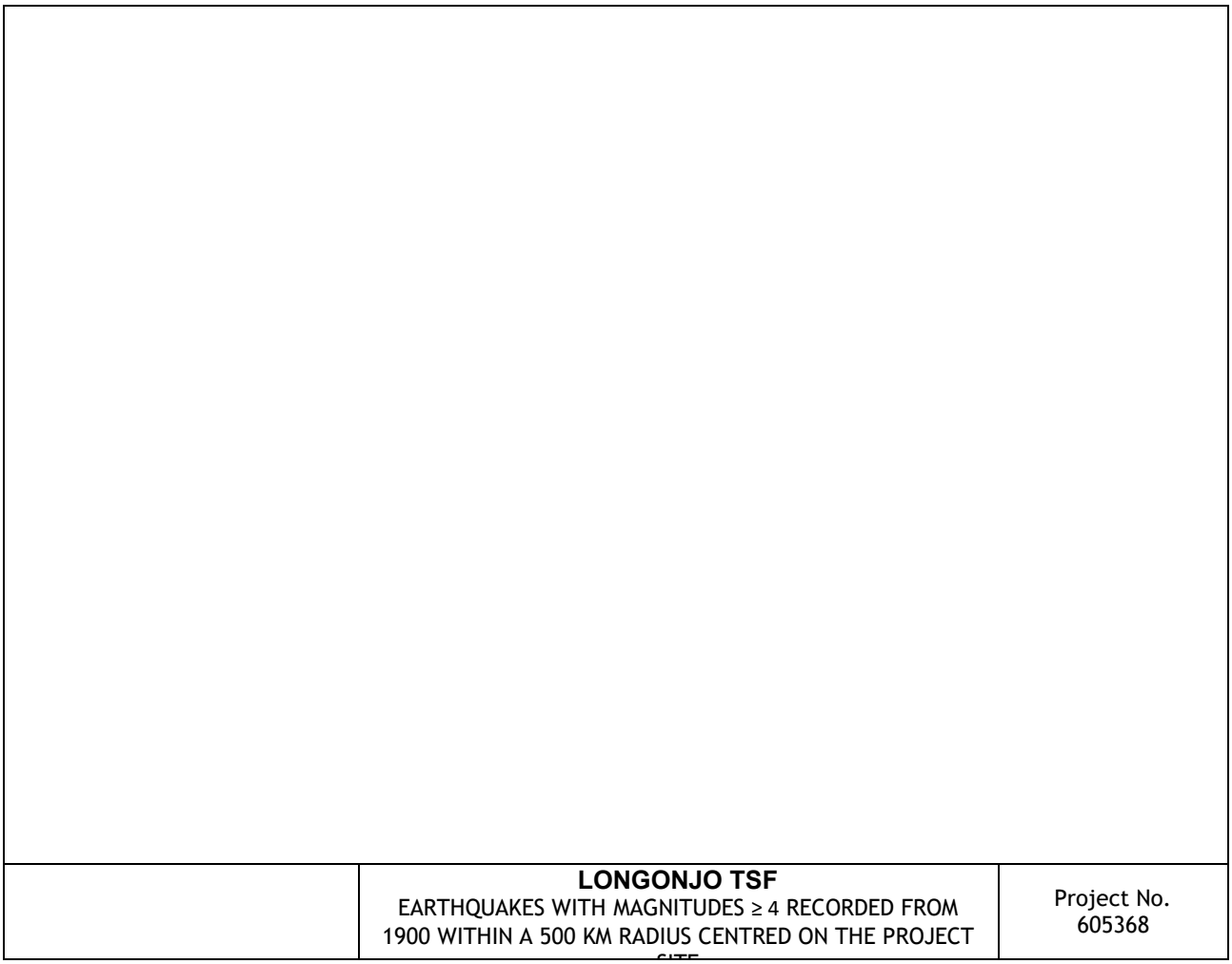

Figure 1-6: Earthquakes with magnitudes ≥ 4 recorded from 1900 within a 500 km radius centred on the project site.

Table 1-1: ISC Bulletin events with magnitude ≥ 4 within 500 km of the site

Date	Time	Latitude	Longitude	Depth (km)	Author	Magnitude Type	Magnitude	Distance to TSF COMP 1 & 2 (km)	Distance to TSF COMP 3 (km)
24/05/1914	15:56:24	-10	15	35	PAS	MS	6	325	327
09/07/1968	00:13:35	-10.6658	12.1393	10	ISC	mb	4.2	418	421
12/08/1968	09:48:23	-10.3285	13.4648	10	USCGS	mb	4.4	345	348
01/09/1968	21:07:51	-15.8345	12.9506	10	BUL	M	4.1	402	404
07/12/1974	16:32:55	-13.75	14.7109	10	BUL	M	4.6	105	106
22/02/1976	07:12:11	-11.1299	12.3398	25.8	ISC	mb	5	370	374
09/05/1979	07:29:43	-14.3638	14.002	10	ISC	mb	4.8	205	206
24/07/1982	20:40:12	-13.4026	14.314	10	BUL	M	4.1	109	112
26/11/1987	04:54:09	-16.7413	13.8199	10	NEIC	mb	4.4	447	447
05/06/1989	16:23:41	-11.9056	14.7149	7.8	ISC	mb	5.1	125	128
20/11/1996	01:36:18	-10.1485	13.3685	10	ISC	mb	4.1	367	370
23/03/2003	18:09:26	-13.8379	14.344	27.8	NEIC	mb	4.8	136	138
13/12/2004	10:26:48	-10.3093	12.3888	10	IDC	mb1	4.3	422	426
18/06/2007	15:35:07	-13.8129	14.699	10	IDC	mb1	4.3	111	112
19/11/2013	00:15:21	-11.8675	14.7391	10	NEIC	mb	4.2	128	131
10/11/2014	01:28:55	-12.5513	14.9736	10	IDC	mb1	4.1	49	52
14/10/2016	00:32:48	-15.3534	12.0428	10	PRE	mb	4.6	433	436
05/10/2018	15:48:23	-11.1601	12.2675	10	NEIC	mb	4.3	375	379
31/08/2023	09:27:43	-13.4454	17.2497	10	GFZ	mb	4.8	229	225
26/04/2024	17:22:44	-9.7347	15.5113	10	NEIC	mb	4.2	355	356
15/05/2024	14:57:10	-15.139	15.742	10	BUL	MD	4.8	251	249
05/06/2024	08:42:24	-13.711	14.249	10	GCMT	MW	4.9	134	136
28/10/2024	15:25:03	-16.0295	14.8982	0	NEIC	mb	4.3	344	343

Source: ISC Bulletin.

Note: Data on or after 2023/11/01 have not been reviewed by the ISC.

1.1.5. Local faulting at the site

The project site appears to lie within the Lucapa basement fault zone and is shown in Figure 1-7. The Lucapa basement fault zone trends in a 050-060° direction and extends over 1 600 km across the Congo craton (White et al., 1995, cited in Guiraud et al., 2010). The 50-90 km wide Lucapa corridor hosts Early to Late Cretaceous age (Skinner et al., 1992, cited in Guiraud et al., 2010) kimberlite and carbonatite pipes and dykes at the intersection between the northeast-southwest and northwest-southeast structural trends that disrupt the Angolan shield (White et al., 1995, cited in Guiraud et al., 2010). The Lucapa fault zone can be traced to the southwest to the transforms of the Mid Atlantic Ridge (Sykes, 1978, cited in White et al., 1995). Within the Lucapa zone, the fault and fracture trends are east-northeast, which corresponds to the internal R-shear for a dextral sense of displacement (White, et al., 1995). Guiraud et al. (2010) suggest a link between the Benguela sinistral transform rift and deep-seated hotspot magmatism in the continental interior, based on the emplacement of the Angolan kimberlites along the Lucapa corridor. The offshore transform faults, i.e., the Rio de Janeiro, Benguela, and Lucapa FZs, may connect with the onshore intracontinental transform faults, and oceanwards, with major oceanic transform fracture zones where they control major offsets in the continental/oceanic crustal boundary based on the offset of gravity anomalies (Guiraud, et al., 2010). Multiple, M≥ 4 seismic events occur within a 500 km radius of the project site, which are shown in

Figure 1-7, and structural features that are in proximity to M ≥ 4 seismic events, which are within a 500 km radius of the project site, are listed in Table 1-2. Locally, within a 100 km radius centred on the project site, the fault and shear zones trending in a NE-SW direction are shown in Figure 1-8, with mapped faults (Angola Geologic Map 1: 1 000 000, cited in Neto et al., 2018; IICP - Laboratorio Nacional de Investigação Científica Tropica (Instituto de Investigação Científica Tropical), 2011), having a similar trend.

Figure 1-7: Mapped faults, magnetic and tectonic structures, Precambrian shear zones and fault zones, and tectonic-magmatic reactivation zones from literature sources (Escosa et al., 2024; Rey-Moral et al., 2022; Guiraud et al., 2010; Neto et al., 2018; IICP - Laboratorio

Nacional de Investigação Científica Tropica (Instituto de Investigação Científica Tropical), 2011; Pereira et al., 2003), and earthquakes with magnitude ≥ 4 within a 500 km radius centred on the project site.

Table 1-2: Structural features in proximity to M ≥ 4 seismic events within a 500 km radius of the project site

Fault name	M	Fault type	Trend	Length (km)	Distance (km) from event to TSF COMP 1 & 2	Distance (km) from event to TSF COMP 3
Main faults (Pereira et al., 2013)	4.3 mb	-	312	182	344	343
Major Precambrian fault zone (Guiraud et al., 2010)	4.3 mb	-	059	544	111	112
N010 Paleoproterozoic Eburnean shear zones (Escosa et al., 2024)	6 Ms	-	N010	24	325	327
Mapped faults (Angolan Geological Map 1:1 000 000) (Neto et al., 2018)	5.1 mb	-	084	34	125	128
Falha (Fault?) (IICP - Laboratorio Nacional de Investigação Científica Tropica (Instituto de Investigação Científica Tropical), 2011)	4.9 MW	-	043	88	134	136

Figure 1-8: Mapped faults, magnetic and tectonic structures, Precambrian shear zones and fault zones, and tectonic-magmatic reactivation zones from literature sources (Escosa et al., 2024; Guiraud et al., 2010; Neto et al., 2018; IICP - Laboratorio Nacional de Investigação Científica Tropica (Instituto de Investigação Científica Tropical), 2011; Pereira et al., 2003) and earthquakes with magnitude ≥ 4 within a 100 km radius centred on the project site.

2. Conclusions

The project site lies within the Congo craton, which is considered a stable continental region and is characterised by low levels of seismic activity.

Salt tectonics, due to depositional loading by clastics derived from the uplifted areas, that intensified Cenozoic gravity-induced rafting of slabs of the post-salt succession downdip along the Aptian salt

decollement, occur within the Outer Kwanza Basin, and have active fault systems, which are within a 500 km radius centred on the project site.

Locally, the project site appears to lie within the Lucapa basement fault zone or Lucapa corridor, which is dominated by Precambrian fault and shear zones. Although it is not clear if these faults or shear zones are active, there is potential for brittle reactivation of preexisting basement-rooted faults based on Nkodia et. al (2022)'s remark for potential reactivation based on the clustering of intraplate earthquakes along or around preexisting basement-rooted faults. Intraplate faults could be activated by far-field strain transfer from transform faults along the spreading ridges of the Mid-Atlantic Ridge, considering that some of the oceanic fracture zones are active.

Yours faithfully,

SRK Consulting (South Africa) (Pty) Ltd

[Author name (Registration)]
[Title]

[Reviewer/Project Manager (Registration)]
[Title]

[Reviewer/Partner (Registration)]
[Title]

Disclaimer

The opinions expressed in this Report have been based on the information supplied to SRK Consulting (South Africa) (Pty) Ltd (SRK). SRK has exercised all due care in reviewing the supplied information. Whilst SRK has compared key supplied data with expected values, the accuracy of the results and conclusions from the review are entirely reliant on the accuracy and completeness of the supplied data. SRK does not accept responsibility for any errors or omissions in the supplied information and does not accept any consequential liability arising from commercial decisions or actions resulting from them. Opinions presented in this report apply to the site conditions and features as they existed at the time of SRK's investigations, and those reasonably foreseeable. These opinions do not necessarily apply to conditions and features that may arise after the date of this Report, about which SRK had no prior knowledge nor had the opportunity to evaluate.

3. References

Alessio, B. L. et al., 2019. Neoproterozoic tectonic geography of the south-east Congo craton in Zambia as deduced from the age and composition of detrital zircons. *Geoscience Frontiers,* Volume 10, pp. 2045-2061.

Ambraseys, N. N. & Adams, R. D., 1991. Reappraisal of Major African Earthquakes, South of 20°N, 1900-1930. *Natural Hazards,* Volume 4, pp. 389-419.

Erdi, A. & Jackson, C. A.-L., 2022. Salt-Detached Strike-Slip Faulting, Outer Kwanza Basin, Offshore Angola. *Tectonics,* Volume 41, pp. 1-25.

Escosa, F. O. et al., 2024. Mode of extension and final architecture of the south Angolan margins controlled by Precambrian lithospheric heterogeneity. *Marine and Petroleum Geology,* 161(106637), pp. 1-29.

Guiraud, M., Neto-Buta, A. & Quesne, D., 2010. Segmentation and differential post-rift uplift at the Angola margin as recorded by the transform-rifted Benguela and oblique-to-orthogonal-rifted Kwanza basins. *Marine and Petroleum Geology,* Volume 27, pp. 1040-1068.

Gutenberg, B. & Richter, C. F., 1944. Frequency of Earthquakes in California. Bulletin of the Seismological Society of America. *Seismological Society of America,* Volume 34, p. 185–88.

IICP - Laboratorio Nacional de Investigação Científica Tropica (Instituto de Investigação Científica Tropical), 2011. *SASSCAL Data and Information Portal.* [Online]
Available at: http://data.sasscal.org//metadata//view.php?view=geodata&id=289
[Accessed 10 11 2025].

International Seismological Centre, 2025. International Seismological Centre.

Klöcking, M. et al., 2020. A tale of two domes: Neogene to recent volcanism and dynamic uplift of northeast Brazil and southwest Africa. *Earth and Planetary Science Letters,* Volume 547, p. 116464.

Letamo, A., B, K. & Tezeswi, T. P., 2023. Seismicity pattern of African regions from 1964-2022: b-value and energy mapping approach. *Geomatics, Natural Hazards and Risk,* 14(1), p. 197104.

Megharaoui, M. et al., 2016. The Seismotectonic Map of Africa. *Episodes,* 39(1), pp. 9-18.

Neto, F. A. P. et al., 2018. Angola seismicity. *Journal of Seismology,* Volume 22, p. 1113–1126.

Nkodia, H. M. D.-V. et al., 2022. Seismogenic Fault Reactivation in Western Central Africa: Insights From Regional Stress Analysis. *Geochemistry, Geophysics, Geosystems,* pp. 1-23.

Pereira, E., Rodrigues, J. & Reis, B., 2003. Synopsis of Lunda geology, NE Angola: Implications for diamond exploration. *Comunicações do Instituto Geológico e Mineiro,* Volume 90, pp. 189-212.

Rey-Moral, C. et al., 2022. Recording the largest gabbro-anorthositic complex worldwide: The Kunene Complex (KC), SW Angola. *Precambrian Research,* Volume 379, p. 106790.

Schirbel, L., Assumpcao, M., Neto, F. A. P. & Franca, G. S., 2024. Induced seismicity at the Laúca reservoir, Angola Craton: Focal mechanisms and implications for the stress field in Western Central Africa. *Journal of African Earth Sciences,* 215(105327), pp. 1-10.

White, S. H., de Boorder, H. & Smith, C. B., 1995. Structural controls of kimberlite and lamproite emplacement. *Journal of Geochemical Exploration,* Volume 53, pp. 245-264.